Supporting Information

Koh et al. 10.1073/pnas.1424850112

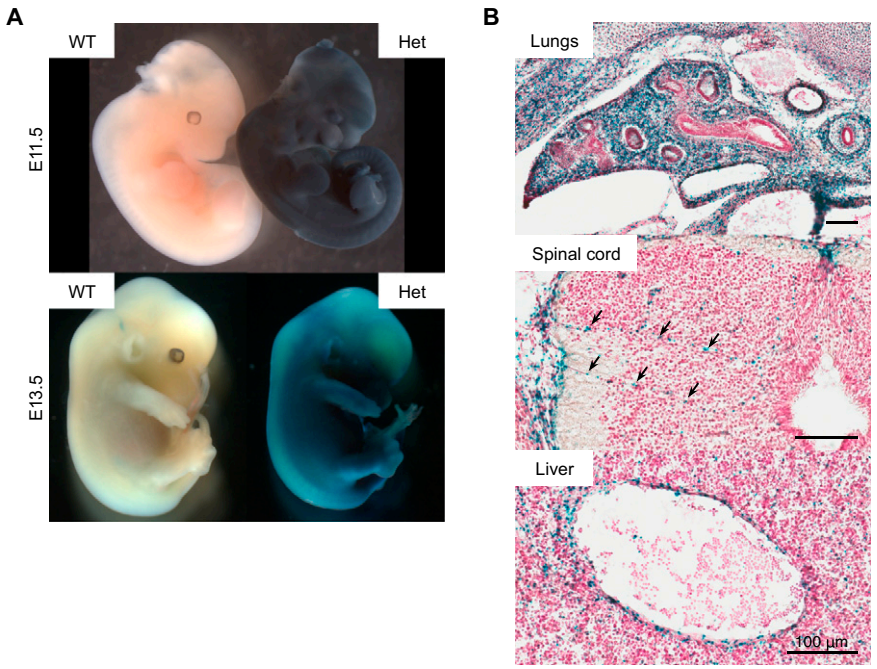

Fig. S1. *Chd1* is broadly expressed in the midgestational mouse embryo. Related to Fig. 1. (*A*) Whole-mount X-gal staining of $Chd1^{LacZ}$ embryos indicates a broad expression of *Chd1* in E11.5 and E13.5 embryos. (*B*) $Chd1^{LacZ}$ is expressed in the endothelium in various tissues in the E13.5 embryo, including in the lungs, intramedullary blood vessels in the spinal cord (black arrows), and the ductus venosus in the FL. (Scale bars, 100 μm.)

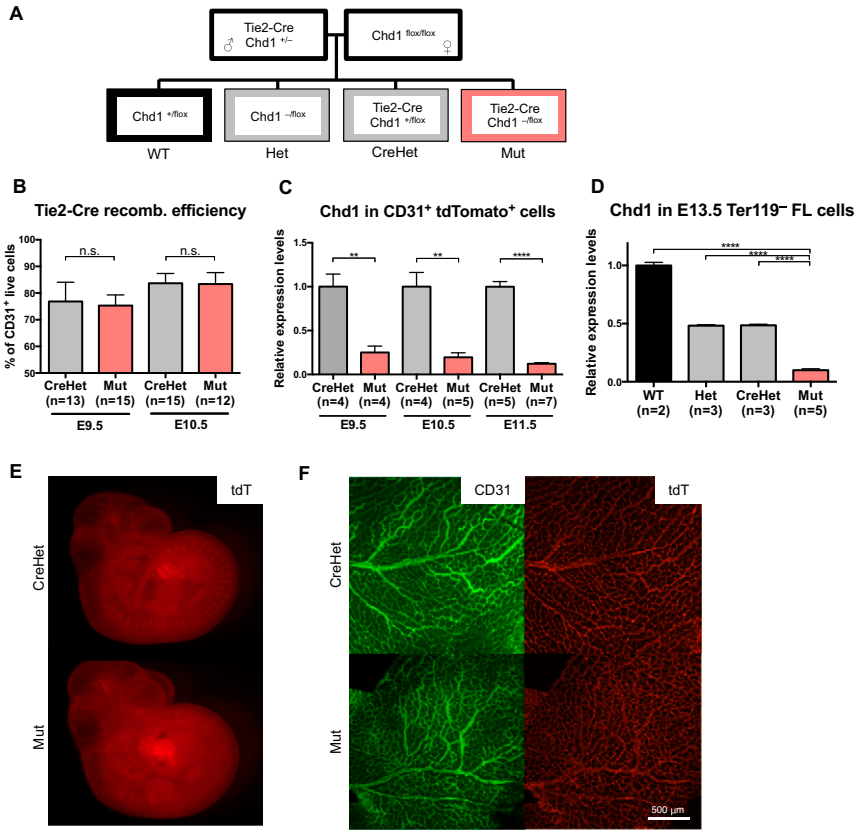

Fig. S2. High recombination efficiency and normal development of the vasculature in endothelial *Chd1* mutants. Related to Fig. 1. (*A*) Mouse breeding scheme used to generate *Tie2-Cre; Chd1*$^{-/flox}$ mutant embryos. One in four embryos is expected to be of the mutant genotype. (*B*) Tie2-Cre is an efficient Cre deletor line, achieving 76% recombination in E9.5 CD31^{+} cells and a significantly higher 84% at E10.5 ($P < 0.0001$). Recombination efficiency is not significantly different between CreHet controls and mutants at either stage. (*C* and *D*) qRT-PCR analyses document the loss of *Chd1* expression in CD31^{+} tdTomato^{+} cells at E9.5, E10.5, and E11.5 and in E13.5 Ter119^{-} FL cells. Error bars indicate SEM. $^{**}P \leq 0.01$; $^{****}P \leq 0.0001$; n.s., not significant. (*E*) tdTomato reporter marks the extensive Cre recombination within the embryonic vasculature in E11.5 embryos. (*F*) Whole-mount immunofluorescence of E10.5 CreHet and mutant yolk sacs shows a normal endothelial network.

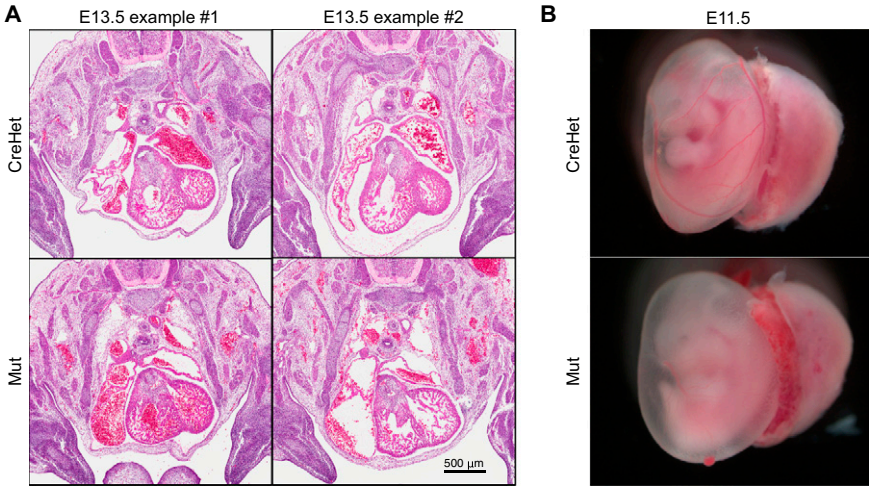

Fig. S3. Normal heart development but evidence of anemia in endothelial *Chd1* mutants. Related to Fig. 1. (*A*) Four-chamber heart view; transverse sections of CreHet and mutant hearts at E13.5 show no visible defects in heart chamber formation. (*B*) Yolk sacs of mutant E11.5 embryos appear anemic immediately after removal from the decidua.

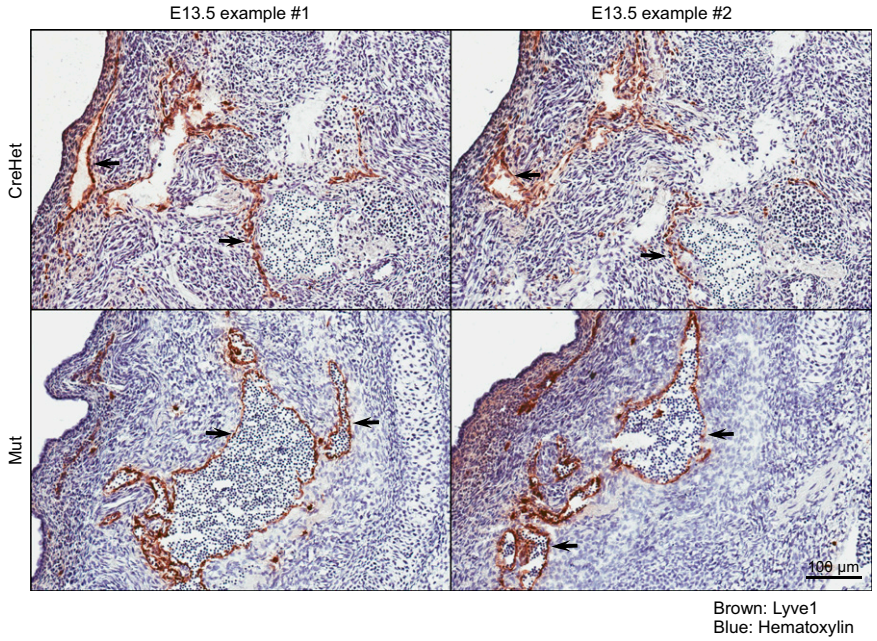

Fig. S4. Endothelial *Chd1* mutants display blood within lymphatic vessels. Related to Fig. 1. Immunohistochemical staining of Lyve1 marks lymphatic vessels (arrows) that appear collapsed or open but devoid of blood cells in CreHet control. These vessels are enlarged and filled with blood cells in endothelial *Chd1* mutants.

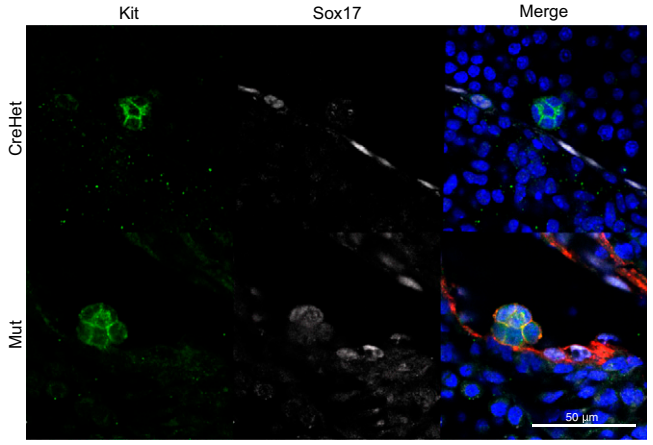

Fig. S5. *Chd1* mutant hemogenic clusters express Kit. Related to Fig. 4. Intraaortic clusters in the E10.5 mutant AGM show proper expression of Kit in *Chd1* mutants.

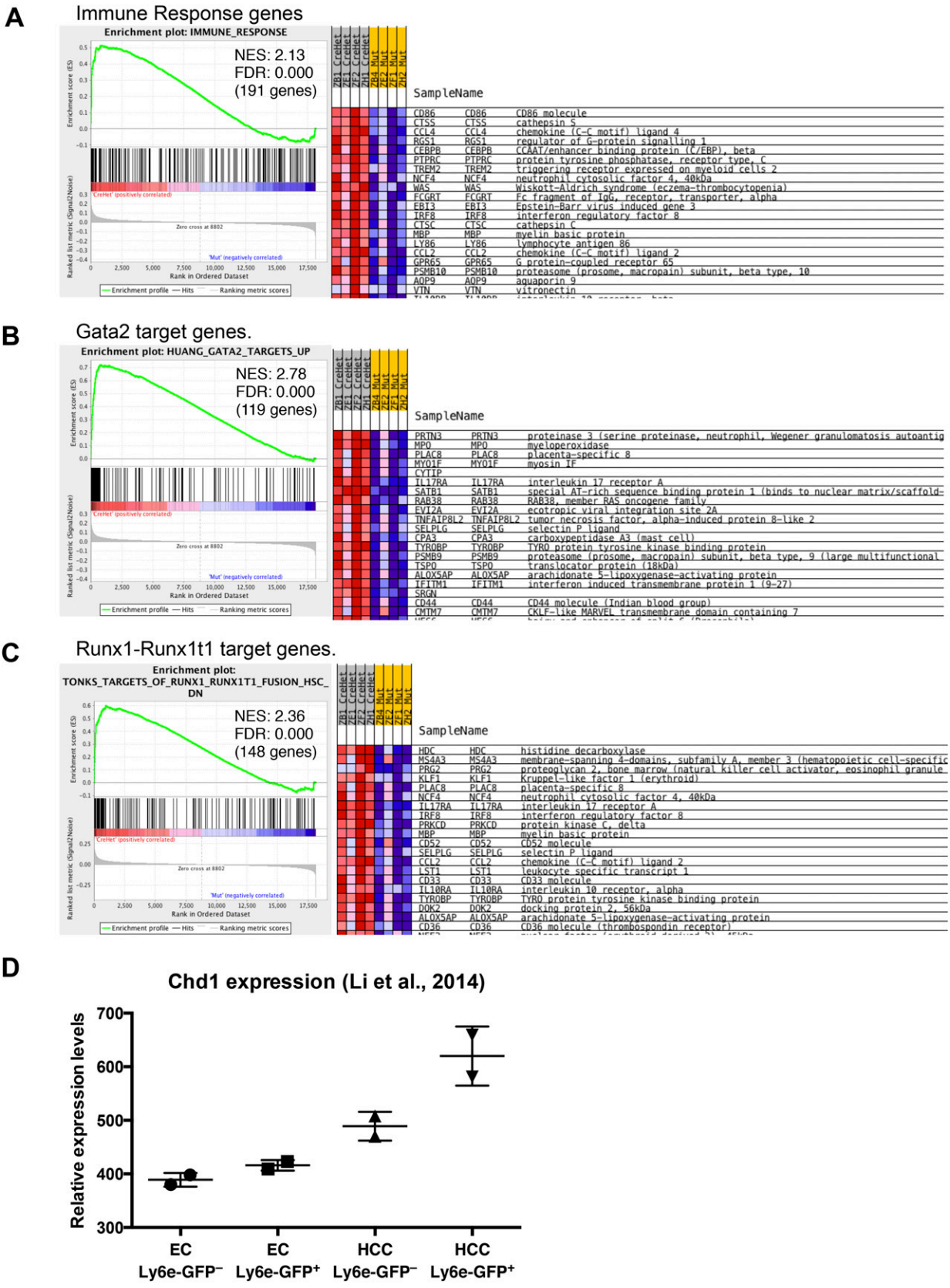

Fig. S6. Hematopoietic and growth genes are down-regulated in *Chd1* mutant endothelium. Related to Fig. 5. (*A*) GSEA for genes annotated with the GO term "immune response." (*B*) GSEA for genes up-regulated in G1ME cells upon knockdown of *Gata2* by RNAi (1). (*C*) GSEA for genes down-regulated in normal hematopoietic progenitors by Runx1-Runx1t1 fusion (2). (*D*) Microarray data from Li et al. (3) show an elevated expression of *Chd1* in hematopoietic cluster cells (HCCs) compared with endothelial cells (ECs). FDR, false discovery rate; NES, net enrichment score. Error bars, SD.

1. Huang Z, et al. (2009) GATA-2 reinforces megakaryocyte development in the absence of GATA-1. *Mol Cell Biol* 29(18):5168–5180.
2. Tonks A, et al. (2007) Transcriptional dysregulation mediated by RUNX1-RUNX1T1 in normal human progenitor cells and in acute myeloid leukaemia. *Leukemia* 21(12):2495–2505.
3. Li Y, et al. (2014) Inflammatory signaling regulates embryonic hematopoietic stem and progenitor cell production. *Genes Dev* 28(23):2597–2612.

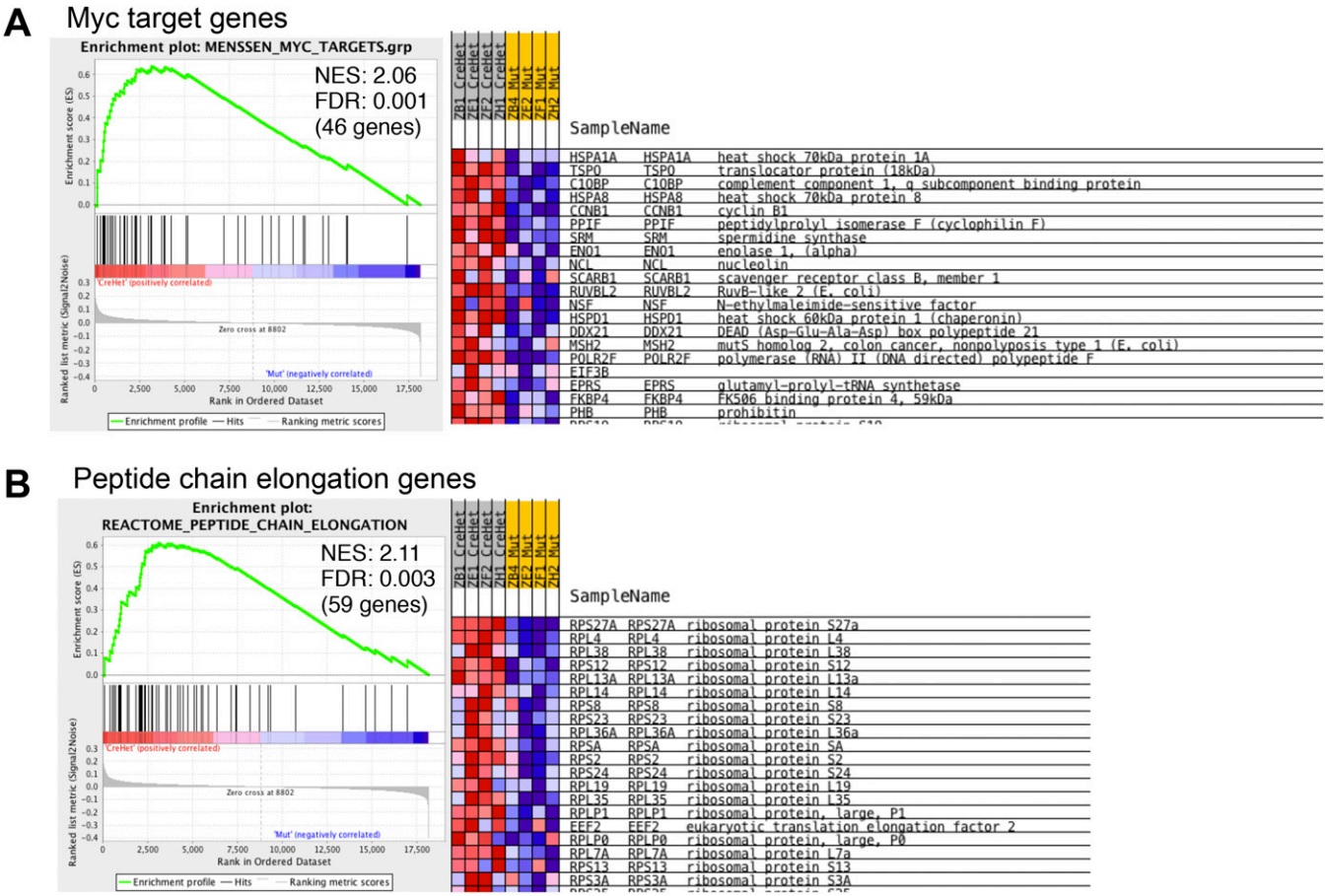

Fig. S7. Myc target genes and translation-related genes are down-regulated in *Chd1* mutant endothelium. Related to Fig. 6. (*A*) GSEA for genes up-regulated by adenoviral expression of Myc in human umbilical vein endothelial cells (HUVEC) cells (1). (*B*) GSEA for genes involved in peptide chain elongation as annotated in the Reactome Pathway Database (www.reactome.org).

1. Menssen A, Hermeking H (2002) Characterization of the c-MYC-regulated transcriptome by SAGE: Identification and analysis of c-MYC target genes. *Proc Natl Acad Sci USA* 99(9):6274–6279.

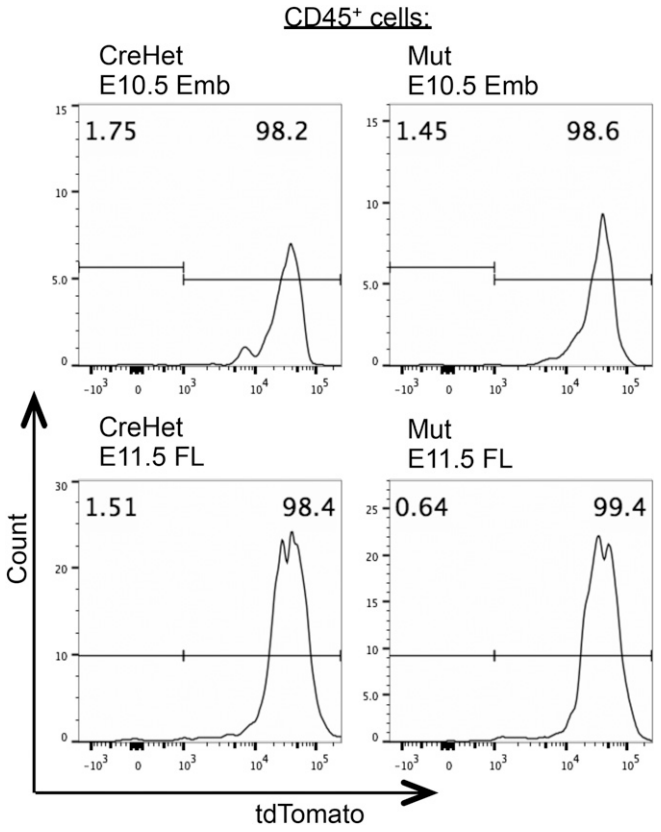

Fig. S8. Vav-Cre is very efficient in hematopoietic cells during development. Related to Fig. 7. Both CreHet controls (*Left*) and *Chd1* mutants (*Right*) generated using Vav-Cre have very high levels of recombination in CD45$^+$ hematopoietic cells in E10.5 whole embryo (*Top*) and E11.5 fetal liver (*Bottom*).

Table S1. List of antibodies used in this study

Antibody	Company	Catalog no.	Host isotype	Clone	Conjugate
Anti-goat secondary	Invitrogen	A21447	Donkey	N.A.	Alexa 647
Anti-rabbit secondary	Invitrogen	A21206	Donkey	N.A.	Alexa 488
Anti-rat secondary	Invitrogen	A21208	Donkey	N.A.	Alexa 488
Anti-rat secondary	Invitrogen	A21209	Donkey	N.A.	Alexa 594
CD117 (Kit)	BioLegend	105812	Rat IgG2b, κ	2B8	APC
CD117 (Kit)	BD Pharmingen	553352	Rat IgG2b, κ	2B8	N.A.
CD11b	BioLegend	101216	Rat IgG2b, κ	M1/70	PE-Cy7
CD19	BioLegend	115530	Rat IgG2a, κ	6D5	APC-Cy7
CD31 (PECAM-1)	BioLegend	102506	Rat IgG2a, κ	MEC13.3	FITC
CD31 (PECAM-1)	BioLegend	102418	Rat IgG2a, κ	390	PE-Cy7
CD31 (PECAM-1)	BD Pharmingen	553370	Rat IgG2a, κ	MEC13.3	N.A.
CD4	BioLegend	100548	Rat IgG2a, κ	RM4-5	BV605
CD45 (LCA)	BioLegend	103116	Rat IgG2b, k	30-F11	APC-Cy7
CD45 (LCA)	BioLegend	103122	Rat IgG2b, k	30-F11	Alexa 488
CD45 (LCA)	BioLegend	103114	Rat IgG2b, k	30-F11	PE-Cy7
CD45 (LCA)	BioLegend	103132	Rat IgG2b, κ	30-F11	PerCP-Cy5.5
CD8	BioLegend	100733	Rat IgG2a, κ	53–6.7	PerCP-Cy5.5
Cleaved caspase 3	Cell Signaling	9661	Rabbit	Asp175	N.A.
Ly-6A/E (Sca-1)	BioLegend	108108	Rat IgG2a, κ	D7	PE
Ly-6G (Gr-1)	BD Biosciences	553127	Rat IgG2b, κ	RB6-8C5	FITC
NK1.1	BioLegend	108708	Mouse IgG2a, κ	PK136	PE
Runx1, 2, 3	Abcam	Ab92336	Rabbit IgG	EPR3099	N.A.
Sox17	R&D Systems	AF1924	Goat IgG	Q9H6I2	N.A.
TCRβ	BioLegend	109212	Armenian hamster IgG	H57-597	APC
TER-119	BioLegend	116228	Rat IgG2b, κ	TER-119	PerCP-Cy5.5
TER-119	BioLegend	116208	Rat IgG2b, κ	TER-119	PE

N.A., not applicable.

Table S2. List of qRT-PCR primers used in this study

Gene	F/R	Sequence, 5′-3′	Notes
Ubb	F	GCGGTTTGTGCTTTCATCAC	Housekeeping for mRNA detection
	R	GGCAAAGATCAGCCTCTGCT	
L7	F	AGCGGATTGCCTTGACAGA	Housekeeping for mRNA detection
	R	AACTTGAAGGGCCACAGGAA	
GAPDH	F	AGGTCGGTGTGAACGGATTTG	Housekeeping for mRNA detection
	R	TGTAGACCATGTAGTTGAGGTCA	
Fabpi-200	F	TGGACAGGACTGGACCTCTGCTTTCCTAGA	Housekeeping for genomic DNA detection
	R	TAGAGCTTTGCCACATCACAGGTCATTCAG	
Fabpi-500	F	CCTCCGGAGAGCAGCGATTAAAAGTGTCAG	Housekeeping for genomic DNA detection
	R	TAGAGCTTTGCCACATCACAGGTCATTCAG	
Chd1-flox allele	F	CGGAACCGAAGTTCCTATTCCGAAGTTCCT	Detection of intact *Chd1* flox allele
	R	CCGCCTACTGCGACTATAGAGATATCAACC	
Chd1 exon15-16	F	CAAGGAGCTTGAGCCATTTC	Detection of *Chd1* mRNA levels
	R	TGGTGGTTTAATGAGGTAGCAA	
ζ-Globin	F	TGGATTCTGTGTGGGACTAAGGC	Globin primers (1)
	R	GGGCTTGGTGGGACTGTAAGG	
α1/α2-Globin	F	GCACAACCCAGCCCCAGAAT	
	R	ACACGCCCTTGGAGCAGTTC	
εγ-Globin	F	CCAGACTTGCCATCATGGTGA	
	R	TCACCACCAACCTCTTCAACAT	
βH1-Globin	F	GGACAGGTCTTCAGCCTCTTGA	
	R	CAGATGCTTGTGATAGCTGCCT	
β1-Globin	F	CACCGAAGCCTGATTCCGTAGA	
	R	GAAGCAAATGTGAGGAGCAACTGA	
β2-Globin	F	TGGTTGTCATCTCTGAAGCCTCAC	
	R	CTGCCCACTCTGTCCTCTCTGA	

F, forward; R, reverse.

1. Kingsley PD, et al. (2006) "Maturational" globin switching in primary primitive erythroid cells. *Blood* 107(4):1665–1672.

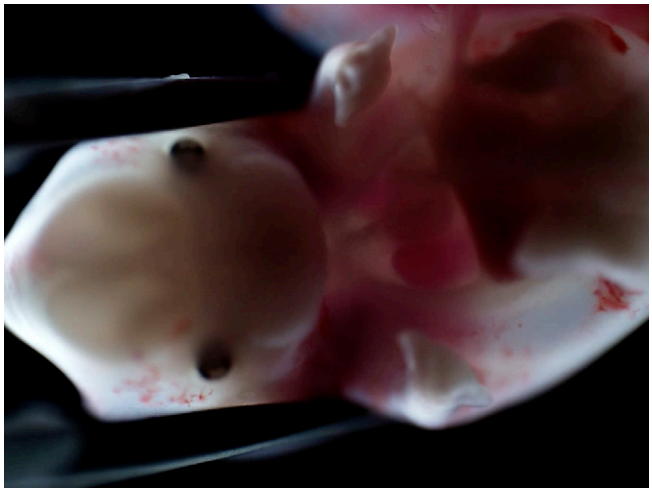

Movie S1. Related to Fig. 1. Mutant E13.5 embryo displays beating heart and blood flow within embryonic and umbilical vessels despite severe anemia.

Movie S1

Other Supporting Information Files

Dataset S1 (TXT)